Nanostructures

DOI: 10.1002/anie.200802570

Optical Waveguide Based on Crystalline Organic Microtubes and Microrods**

*Yong Sheng Zhao, Jinjie Xu, Aidong Peng, Hongbing Fu, Ying Ma, Lei Jiang, and Jiannian Yao**

During the past decade, ever increasing attention has been paid to one-dimensional (1D) nano- and microstructured materials because of their potential applications as building blocks for miniaturized devices, such as logic gates,[1] photodetectors,[2] and chemical sensors.[3] In the past couple of years, 1D materials have begun to serve as optical guides,[4] which are capable of propagating and manipulating light efficiently on the subwavelength scale. Nano- to microsized optical waveguides are important interconnectors, and great effort has been paid to develop optical waveguides based on 1D inorganic nanostructures. Recently, it was realized that 1D nano- and microstructures based on polymers[5] and small organic compounds[6] could also serve as effective building blocks to generate and propagate light in future miniaturized optoelectronics. In addition, 1D organic materials, especially crystalline ones,[7] have many unique photonic and electronic properties[8] because of their weak intermolecular interactions[9] and high luminescence efficiency.

Up until now, research on both organic and inorganic 1D nanoscale waveguides has focused on solid structures, including nanowires and ribbons, while much less attention has been paid to hollow tubular structures. Tubular 1D structures are expected to display different waveguide behaviors from the solid ones because of the air inside them. Herein, we report on the preparation of two kinds of crystalline microstructures, that is, tubes and rods, from a small organic compound. The selected model compound 9,10-bis(phenylethynyl)anthracene (BPEA, Figure 1) is a green light-emitting dye, which has had a wide variety of applications because of its good solubility, thermal stability, and especially its remarkably high emission efficiency (with a fluorescence quantum yield of higher than 0.9).[10] A facile method that combines reprecipitation[11] and self-assembly techniques was developed to fabricate the single-crystalline BPEA microtubes, while the BPEA microrods were prepared by a solvent volatilization method. Characterization of the single tubes and rods indicates that the 1D BPEA microstructures can serve as active optical waveguides that allow locally excited photoluminescence to propagate along the length of the 1D structures and outcouple at the tube/rod tips. The tubular structures reveal lower optical loss than the solid rods during propagation of light. The optical loss in the microtubes is mainly from reabsorption, while the predominant sources of loss for the microrods are scattering and coupling between the rods and the substrates.

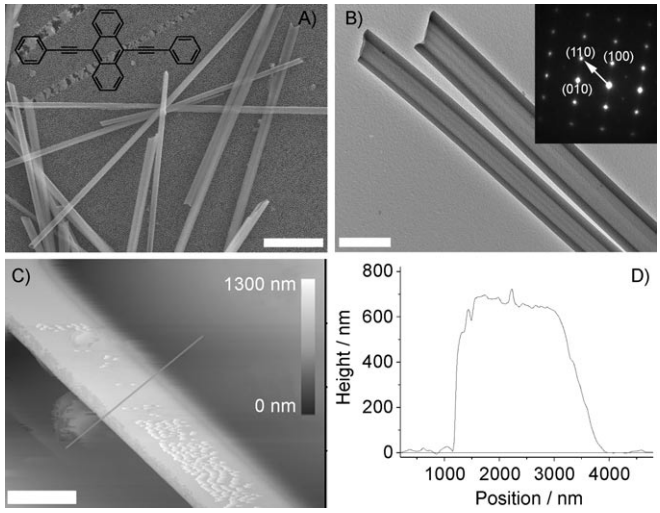

Figure 1. A) SEM image of the BPEA microtubes, scale bar: 10 μm. Inset: the chemical structure of a single BPEA molecule. B) TEM image of some typical BPEA microtubes, scale bar: 2 μm. Inset: SAED pattern, the arrow indicates the direction of the tube. C) AFM image of a single microtube, scale bars: 2 μm. D) Cross-section along the gray line in (C).

The BPEA microtubes were prepared by a method that combined reprecipitation and self-assembly. In brief, a stock solution of BPEA in ethanol (10^{-3} M) was injected rapidly into 10 mL of boiling ultrapure water under vigorous agitation. The boiling system was subsequently refluxed for 30 minutes and then cooled to room temperature at different rates. The change in the solvent conditions in these two processes induces the nucleation and self-assembly of BPEA into microtubes. Figure 1 A and B illustrate the typical SEM and TEM images of the BPEA microtubes. These images indicate that the microtubes have high monodispersity and that each single tube has a uniform size along its entire length. The selected-area electron diffraction (SAED) pattern reveals

[*] Dr. Y. S. Zhao,[+] A. Peng,[+] H. Fu, Y. Ma, Prof. J. Yao
CAS Key Laboratory of Photochemistry
Institute of Chemistry, Chinese Academy of Sciences
Beijing, 100190 (China)
Fax: (+86) 10-8261-6517
E-mail: jnyao@iccas.ac.cn
Dr. J. Xu,[+] Prof. L. Jiang
CAS Key Laboratory of Organic Solids
Institute of Chemistry, Chinese Academy of Sciences (China)

[+] These authors contributed equally to this work.

[**] This work was supported by the National Natural Science Foundation of China (nos. 50221201, 90301010, and 20733006, 50573084), the National Research Fund for Fundamental Key Project No. 973 (2006CB806200), and the Chinese Academy of Sciences.

Supporting information for this article is available on the WWW under http://dx.doi.org/10.1002/anie.200802570.

that the tubes have a single-crystalline structure and grow along the [110] direction of the BPEA crystal. This was also proved from the contrast of the XRD patterns (see Figure S1 in the Supporting Information), which testifies to the preferential orientation of the (110) lattice planes in the microtubes. AFM was utilized to investigate the topography of the BPEA microtubes. The cross-sections of the tubes were shown to be rectangular (see Figure S2 in the Supporting Information). Figure 1C shows the AFM image of the tubes which have a typical height and width of 690 nm and 2.5 μm, respectively (Figure 1D).

The TOF EI mass spectra proved that the as-prepared microtubes had not undergone chemical reaction during the self-assembly process (see Figure S3 in the Supporting Information). The length and diameter of the as-prepared BPEA microtubes can be readily controlled by altering the preparation conditions. Longer tubes can be obtained by increasing the volume of the injected stock solution. For example, injection of 50, 100, 300, and 500 μL of BPEA ethanol solution at a fixed cooling rate of 5 °C min^{-1} gave microtubes with final lengths of about 10, 30, 60, and more than 100 μm, respectively. Moreover, BPEA microtubes with larger diameters can be prepared by increasing the cooling rate of the boiling system. For example, at a fixed volume of stock solution of 300 μL, cooling rates of 1, 5, 10, and 20 °C min^{-1} resulted in microtubes with diameters of around 1, 2, 3, and 5 μm, respectively.

To investigate the mechanism of formation of the as-prepared BPEA tubular structures, we studied the evolution of their morphology over time (see Figure S4 in the Supporting Information). It was observed that if no reflux was adopted, only solid microrods were obtained. With a prolonging of reflux time, the center parts of the rodlike microstructures were hollowed out from the top of each rod to the middle region. After reflux for about 30 minutes, most of the solid rods were entirely hollow, and perfect microtubes were obtained. From this study, the etching of BPEA molecules in the central region of the solid microrods by the small amount of ethanol during the reflux is considered to be responsible for the formation of the hollow tubular structures. It has been proved[12] that a higher density of defects exists in the core region of crystalline 1D nanomaterials. The vigorous agitation and high-temperature reflux will drive the solvent (ethanol) to penetrate into the central regions of the preformed nanorods and dissolve the BPEA molecules there, which results in the formation of the tubular structures. This mechanism of formation was further proved by the observation of some other intermediate products, in which the BPEA molecules at the center of some solid nanorods had not been etched completely at a shorter reflux time (see Figure S5 in the Supporting Information).

The absorption and photoluminescence (PL) spectra of the BPEA microtubes are shown in Figure 2 along with those of the BPEA monomers in ethanol. The monomers exhibit two resolved absorption bands at 430 and 455 nm. The two bands become less resolved for the microtube samples, and a new band resulting from the aggregation of the BPEA molecules in the microtubes emerges at longer wavelength. The aggregation also results in a red-shift of the PL spectrum

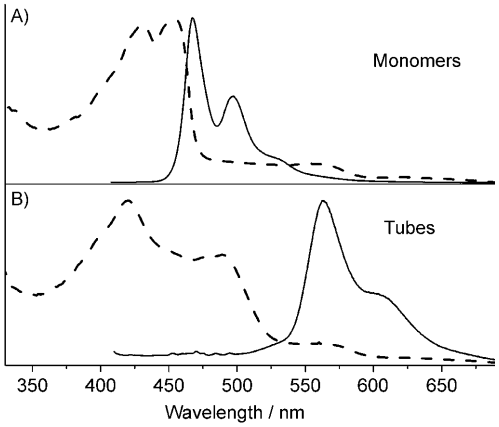

Figure 2. Absorption (dash) and fluorescence (solid) spectra of BPEA monomers in ethanol (top) and BPEA microtubes (bottom).

by as much as 100 nm with respect to that of the monomers, and the emission color changes from green to yellow.

We used PL microscopy to study the optical waveguide properties of the as-prepared micotubes. The PL image shown in Figure 3A indicates that the BPEA tubes exhibit yellow emission, with very bright luminescence spots at both tips and relatively weaker emission from the bodies of the tubes, which is a typical characteristic of an optical waveguide. This finding suggests that the tubes absorb the excitation light and propagates the PL emission toward the tip. Almost all of the observed tubes reveal this kind of waveguide behavior. Figure 3B shows the PL image of two crossed tubes. It reveals that the brighter emission can also be observed from the intersection of the crossed tubes as well as from the ends of each tube. This result indicates that the emission light can also be propagated from one tube to another through the crossing point, which was further proved from the microarea images.

The microarea PL microscopy images and the distance-dependent photoluminescence spectra showing propagation of light through single microtubes were measured with a near-field scanning optical microscope (NSOM, see Figure S6 in the Supporting Information for the setup). The tubes were excited with a focused laser (442 nm) down to the diffraction limit at different local positions along the length of the tubes relative to an NSOM collection tip held stationary over one of their ends. With this technique, the process by which light travels along the tubes can be investigated effectively by moving the excited laser. Figure 3C indicates that the local emission of light from each single microtube under laser excitation was so strong that it could be imaged clearly with a color CCD. Interestingly, the tubes illustrate excellent waveguide properties, and the guided fluorescence can be emitted from both ends of the tubes irrespective of the position of excitation. In general, the emission of light can only be observed at the local area of the excited position in microarea fluorescence images. Here, the localization of the out-coupling light at the ends of each tube is a typical characteristic of strong waveguiding behavior. The waveguided light is generated from the PL within the nanowire, and such wires are classified as active waveguides,[11b] as opposed to passive ones into which light must be coupled with external sources.[13]

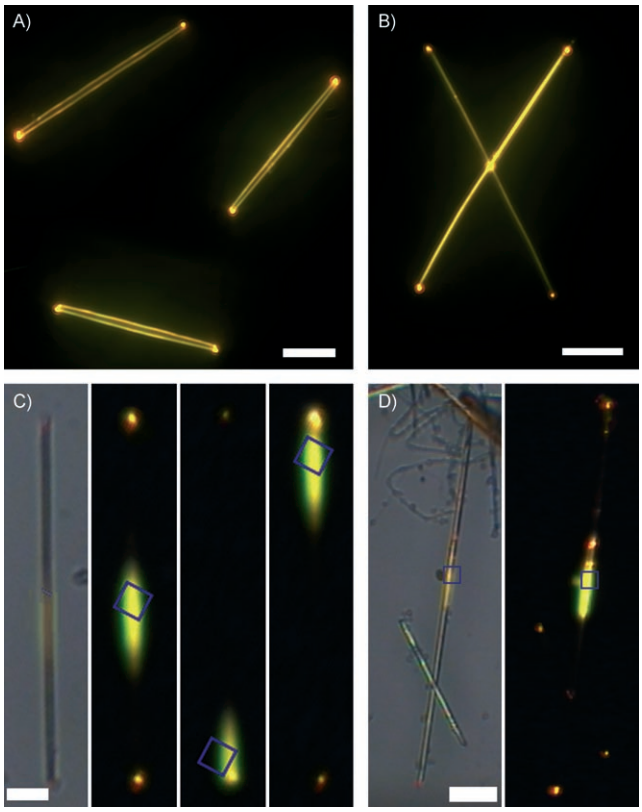

Figure 3. PL microscopy images of A) some isolated BPEA microtubes, and B) two crossed microtubes. Both samples were excited with blue light between 460 and 490 nm. Scale bars: 20 μm. C) Bright-field image, and microarea PL images obtained by exciting identical tubes at three different positions, scale bar: 10 μm. D) Bright-field and microarea PL images of two crossed tubes, scale bar: 20 μm. The blue squares indicate the excited positions.

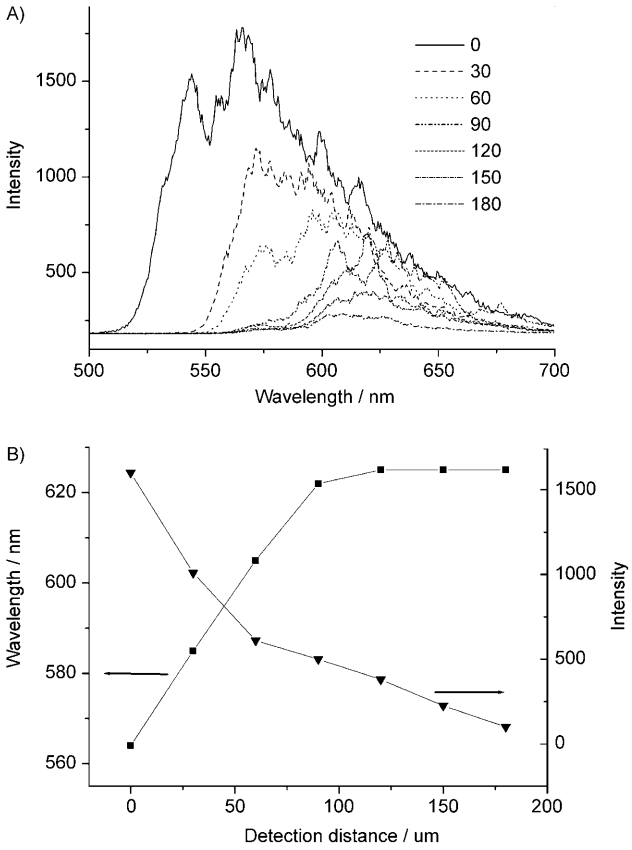

Figure 4. A) Spatially resolved PL spectra of the excited position and out-coupled light by excitation at a distance of 0–180 μm from the end of the tube. The tip intensities were normalized against those measured from the excitation location on the bodies of the tubes. B) Maximum intensity and wavelength versus excitation position for the PL spectra.

More significantly, Figure 3D shows that when the excitation laser is focused on one of the two crossed tubes (also irrespective of the position of excitation), guided emissions can be obtained from the two ends of both tubes as well as from the intersection point, which further testifies to the coupling of light between the crossed tubes. We also observed waveguide behavior in several overlapped tubes, and found that the light can be coupled among multiple tubes irrespective of the intersection angles (see Figure S7 in the Supporting Information).

The spatially resolved near-field PL spectra of the emitted light with respect to the length traveled were measured to gain further insight into the propagation behavior within the BPEA microtubes. Figure 4A shows the locally detected PL spectra with the NSOM collection tip held at the upper terminus and with the excitation laser beam at different points along a single BPEA microtube with a width of 2.5 μm. The plots of peak intensity and wavelength versus excitation position are shown in Figure 4B. The intensities and profiles of the spectra of the excited points do not change substantially with the position along the tube. However, the emissions at the tips exhibit the characteristic property of an active waveguide as the propagation distance increases:[5] First, the intensity of the tip emission decreases almost exponentially with the propagation distance. Second, the tip spectra reveal much greater attenuation in the shorter wavelength region. For example, the emissions below 540 nm are cut off after a propagation of 30 μm, and those below 580 nm are filtered out almost completely by propagation of the light about 90 μm. This finding can be attributed to the reabsorption of the waveguided light during propagation of the PL, which is determined by the absorption behavior of the BPEA microtubes as shown in Figure 2A. There is a considerable absorption from the microtube samples at 540–580 nm, and an even stronger absorption below 540 nm, which will make the tubes self-quench their emissions in these wavelength ranges.

As a result of the reabsorption, the maximum wavelength of the out-coupled emission increases with the increase in the propagation distance when the distance is less than 90 μm. With a further increase of the coupled distance, light of shorter wavelength is filtered out completely, and the maximum emission wavelength is fixed at about 620 nm. In this case, the reabsorption is negligible, considering the low absorption features of the microtubes (Figure 2). However, there are still optical losses with further propagation, with the emission intensity decreasing as the distance increases. Thus,

there must be some other sources for the propagation losses, which will be discussed later.

As a comparison, we also prepared a solid BPEA rodlike microstructure with a square cross-section by a solvent volatilization method. Typically, 1 mL of a saturated solution of BPEA in ethanol was heated to a high temperature and then dropped slowly onto a clean glass wafer. The BPEA rods are obtained on slow evaporation of the solvent. The length and diameter of the rods can be controlled by changing the temperature of the solution. Figure 5 A shows the SEM image of the BPEA microrods prepared at 65 °C. The inset reveals

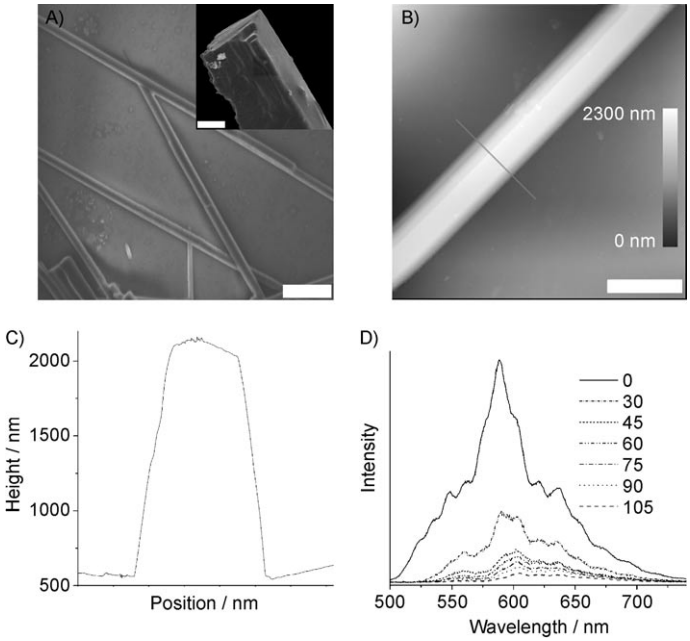

Figure 5. A) SEM image of the BPEA microrods, scale bar: 5 μm. Inset: SEM image of the tip of a single rod. B) AFM image of a single microtube, scale bars: 5 μm. C) Cross-section along the gray line in (B). D) Spatially resolved PL spectra of the excited position and out-coupled light by excitation at a distance of 0–105 μm from the end of the rod.

that the cross-sections of the rods are squares of around 2 × 2 μm^2, which can also be seen from the AFM results shown in Figure 5 B and C. Figure 5 D shows the spatially resolved PL spectra of the waveguided emission out-coupled to the end of the rods. It can be seen from the spectra that the PL intensity decreases by almost a half when propagated over 30 μm in the rods, which is different from that of the BPEA tubes shown in Figure 4. Although the emission spectra overlap to some extent with the absorption, the coupled emission of the rods does not undergo a clear red-shift before a significant decrease in the intensity occurs, which means the optical loss may come from sources other than self-absorption. The evanescent coupling of the guided modes to the underlying substrates may be one possible source.[5b,14] Although we used a quartz wafer with a low refraction index (ca. 1.45), the effect of the substrate can not be avoided, since it is in contact directly with one facet of the rod. The substrate effect is minimized in the case of the tube because there is a layer of air with an even lower refraction index (ca. 1.0) inside the tubes, and, therefore, reabsorption is the predominant contributor to the optical losses. However, Figure 4 indicates that the effect of the substrate on the tubes can not be avoided totally, either. Another possible source for the optical loss in the BPEA microrods is from Rayleigh scattering arising from defects and roughness (see Figure 5 A), which will result in the local variation in the refractive index along the length of the rods. The scattering effect is not very apparent in the microtube samples because the BPEA microtubes are very straight and very smooth on the surfaces, with very few defects, as shown in Figure 1.

To study the possibility of optical losses from scattering in the BPEA microtubes we measured the spatially resolved PL spectra of the waveguided emission out-coupled between more than one tube (see Figure S7 in the Supporting Information). These spectra indicate that before the propagation changes directions to other tubes, the optical loss behavior is similar to that of a single tube waveguide, and reveals a red-shift and a slight decrease in intensity (point b in Figure S7 in the Supporting Information). This result means the optical losses result in this case from reabsorption. For the spectra acquired at the tips of a different tube to the local excitation, the PL intensities decrease significantly with only a small red-shift, as compared with that of the intersection point. This finding is consistent with the case of microrods; thus, the scattering at the intersection points is considered to be responsible for the optical loss, because there is also a variation in the refractive index at the point of intersection.

In summary, we have prepared two kinds of microstructures with rectangular and square cross-sections, respectively, from a low-molecular-weight organic compound (BPEA) and extended the application of miniaturized subwavelength optical waveguides from solid wires and ribbons to hollow tubular structures. The prepared 1D BPEA microstructures can serve as both single tube/rod and intertube/rod active optical waveguides. The air inside the tubes can change the waveguide behavior and helps to reduce the optical loss.

Received: June 2, 2008
Published online: August 11, 2008

Keywords: microscopy · nanostructures · optical waveguide · self-assembly

[1] J. Wang, M. S. Gudiksen, X. Duan, Y. Cui, C. M. Lieber, *Science* **2001**, *293*, 1455.
[2] H. Kind, H. Yan, M. Law, B. Messer, P. Yang, *Adv. Mater.* **2002**, *14*, 158.
[3] Z. L. Wang, *Adv. Mater.* **2003**, *15*, 432.
[4] a) P. Yang, H. Yan, S. Mao, R. Russo, J. Johnson, R. Saykally, N. Morris, J. Pham, R. He, H. J. Choi, *Adv. Funct. Mater.* **2002**, *12*, 323; b) M. Law, D. J. Sirbuly, J. C. Jonhson, J. Goldberger, R. G. Saykally, P. Yang, *Science* **2004**, *305*, 1269; c) A. B. Greytak, C. J. Barrelet, Y. Li, C. M. Lieber, *Appl. Phys. Lett.* **2005**, *87*, 151103; d) A. Pan, D. Liu, R. Liu, F. Wang, X. Zhu, B. Zou, *Small* **2005**, *1*, 980.

[5] a) D. O'Carroll, I. Lieberwirth, G. Redmond, *Nat. Nanotechnol.* **2007**, *2*, 180; b) D. O'Carroll, I. Lieberwirth, G. Redmond, *Small* **2007**, *3*, 1178.
[6] a) K. Takazawa, Y. Kitahama, Y. Kimura, G. Kido, *Nano Lett.* **2005**, *5*, 1293; b) H. Yanagi, T. Morikawa, *Appl. Phys. Lett.* **1999**, *75*, 187; c) F. Balzer, V. G. Bordo, A. C. Simonsen, H. G. Rubahn, *Appl. Phys. Lett.* **2003**, *82*, 10; d) F. Quochia, F. Cordella, A. Mura, G. Bongiovanni, F. Balzer, H. G. Rubahn, *Appl. Phys. Lett.* **2006**, *88*, 041106; e) Y. S. Zhao, A. Peng, H. Fu, Y. Ma, J. Yao, *Adv. Mater.* **2008**, *20*, 1661; f) K. Takazawa, *J. Phys. Chem. C* **2007**, *111*, 8671.
[7] a) Y. S. Zhao, D. Xiao, W. Yang, A. Peng, J. Yao, *Chem. Mater.* **2006**, *18*, 2302; b) Y. S. Zhao, C. Di, W. Yang, G. Yu, Y. Liu, J. Yao, *Adv. Funct. Mater.* **2006**, *16*, 1985; c) Y. S. Zhao, H. Fu, F. Hu, A. Peng, J. Yao, *Adv. Mater.* **2007**, *19*, 3554; d) Y. S. Zhao, H. Fu, F. Hu, A. Peng, W. Yang, J. Yao, *Adv. Mater.* **2008**, *20*, 79.
[8] a) K. Balakrishnan, A. Datar, R. Oitker, H. Chen, J. Zuo, L. Zang, *J. Am. Chem. Soc.* **2005**, *127*, 10496; b) J. K. Lee, W. K. Koh, W. S. Chae, Y. R. Kim, *Chem. Commun.* **2002**, 138; c) Y. S. Zhao, W. Yang, J. Yao, *Phys. Chem. Chem. Phys.* **2006**, *8*, 3300; d) Y. S. Zhao, F. Hu, W. Yang, Y. Ma, H. Fu, J. Yao, *J. Nanosci. Nanotechnol.* **2007**, *7*, 1021;e) Y. S. Zhao, H. Fu, A. Peng, Y. Ma, D. Xiao, J. Yao, *Adv. Mater.* **2008**, *20*, 2859.
[9] a) Y. S. Zhao, W. Yang, D. Xiao, X. Sheng, X. Yang, Z. Shuai, Y. Luo, J. Yao, *Chem. Mater.* **2005**, *17*, 6430; b) Y. S. Zhao, W. Yang, G. Zhang, Y. Ma, J. Yao, *Colloids Surf. A* **2006**, *277*, 111.
[10] a) M. Levitus, M. A. Garcia-Garibay, *J. Phys. Chem. A* **2000**, *104*, 8632; b) A. Zhu, J. O. White, H. G. Drickamer, *J. Phys. Chem. A* **2002**, *106*, 9209.
[11] H. Kasai, H. Kamatani, S. Okada, S. Oikawa, H. Matsuda, H. Nakanishi, *Jpn. J. Appl. Phys.* **1996**, *35*, L221.
[12] a) F. Li, Y. Ding, P. Gao, X. Xin, Z. L. Wang, *Angew. Chem.* **2004**, *116*, 5350; *Angew. Chem. Int. Ed.* **2004**, *43*, 5238; b) X. Zhang, X. Zhang, W. Shi, X. Meng, C. S. Lee, S. T. Lee, *Angew. Chem.* **2007**, *119*, 1547; *Angew. Chem. Int. Ed.* **2007**, *46*, 1525.
[13] L. Tong, R. R. Gattass, J. B. Ashcom, S. He, J. Lou, M. Shen, I. Maxwell, E. Mazur, *Nature* **2003**, *426*, 816.
[14] a) J. C. Johnson, H. Yan, R. D. Schaller, L. H. Haber, R. J. Saykally, P. Yang, *J. Phys. Chem. B* **2001**, *105*, 11387; b) J. C. Johnson, H. Yan, P. Yang, R. J. Saykally, *J. Phys. Chem. B* **2003**, *107*, 8816.

